Electrostatics of Hemoglobins from Measurements of the Electric Dichroism and Computer Simulations

Jan Antosiewicz*‡ and Dietmar Porschke‡

*Department of Biophysics, Warsaw University, 02–089 Warsaw, Poland, and Department of Chemistry, University of Houston, Houston, Texas 77204-5641 USA; ‡Max Planck Institut für biophysikalische Chemie, 37077 Göttingen, Germany

ABSTRACT Hemoglobins from normal human cells, from sickle cells, and from horse were investigated by electrooptical methods in their oxy and deoxy forms. The reduced linear dichroism measured as a function of the electric field strength demonstrates the existence of permanent dipole moments in the range of 250–400 Debye units. The reduced limiting dichroism is relatively small (≤ 0.1); it is negative for hemoglobin from sickle cells and positive for the hemoglobins from normal human cells and from horse. The dichroism decay time constants are in the range from about 55 to 90 ns. Calculations of the electrooptical data from available crystal structures are given according to models of various complexity, including Monte Carlo simulations of proton fluctuations with energies evaluated by a finite difference Poisson-Boltzmann procedure. The experimental dipole moments are shown to be consistent with the results of the calculations. In the case of human deoxyhemoglobin, the root mean square dipole is higher than the mean dipole by a factor of about 4.5, indicating a particularly large relative contribution due to proton fluctuations. The ratio of the root mean square dipole to the mean dipole is much smaller (~ 1.1 to ~ 1.5) for the other hemoglobin molecules. The calculations demonstrate that the dichroism decay time constants are not simply determined by the size/shape of the proteins, but are strongly influenced by the orientation of the dipole vector with respect to the axis of maximal absorbance. The comparison of experimental and calculated electrooptical data provides a useful test for the accuracy of electrostatic calculations and/or for the equivalence of structures in crystals and in solutions.

INTRODUCTION

Electrostatic interactions in proteins are known to be crucial for their structures and functions, but are notoriously difficult to describe quantitatively because of the complexity of protein structures. Because of the long range of electrostatic interactions, virtually all charged residues in proteins interact with each other, leading to a complex mode of coupling (Kirkwood and Shumaker, 1952). The resulting pattern of charged residues usually is not symmetric and leads to an overall electric moment that is accessible to measurements. Thus, experimental dipole moments may be used to check the validity of electrostatic calculations. In the past, dipole moments of proteins have often been characterized by measurements of dielectric relaxation (Oncley, 1943; Grant, 1978). More information may be obtained by measurements of the electric dichroism, because these measurements provide not only the magnitude of the dipole moment but also the optical anisotropy with respect to the dipole vector (O'Konski et al., 1959; Porschke, 1987; Antosiewicz and Porschke, 1989a). Thus, measurements of the electric dichroism provide a more rigorous test for calculations of electrostatic parameters of proteins. In our present investigation, we have characterized several variants of hemoglobins by both measurements and calculations based on available crystal structures. The results demonstrate a reasonable agreement between experiments and calculations. Furthermore, the comparison provides more insight into the nature of the electric moments of large protein molecules.

Received for publication 28 July 1994 and in final form 14 November 1994.

Address reprint requests to Dr. Dietmar Porschke, Max-Planck-Inst. fur Biophysicalische Chem., Karl-Friedrick-Bonhoffer Inst., Am Fassberg 11, D-37077 Gottingen, Germany. Tel.: 49-551-201-438; Fax: 49-551-201-435; E-mail: dpoersc@gwdg.de.

0006-3495/95/02/655/10 $2.00

MATERIALS AND METHODS

All of the hemoglobins were from Sigma Chemical Co. (St. Louis, MO) and were purified by chromatography on Sephadex G25; the purified samples were stored in aliquots at −30°C after rapid freezing in liquid nitrogen. Solutions of oxyhemoglobins were prepared in 10 mM Tris pH 8.0, 100 μM $MgCl_2$, and in 10 mM Tris pH 8.0, 500 μM $MgCl_2$; the samples were saturated with oxygen by bubbling with O_2 for 3 min. Solutions of deoxyhemoglobins were prepared under nitrogen atmosphere with addition of 1 mM $Na_2S_2O_4$ (Di Iorio, 1981). The pH of the samples with added $Na_2S_2O_4$ was slightly decreased to 7.7. Protein concentrations used for measurements corresponded to extinctions in the range from 0.5 to 1.5 measured at 404.7 nm (mercury line used for most electrooptical measurements).

The electric dichroism was measured at 2°C by a pulse generator (Grünhagen, 1974) and an optical detection system (Porschke, 1980) as described. The samples were subjected to field pulses in the range from 10 to 70 kV/cm in a cell with 10 mm optical path length and a distance between the Pt electrodes of 6.05 mm. UV radiation damage was avoided by an automatic shutter for short light pulses synchronized to the field pulses. Both UV transmission and electric field strength as a function of time were transiently stored by a Tektronix 7612D. The stationary changes of light intensity and electric field strength were evaluated by using graphic routines on a LSI 11/23 (Porschke et al., 1984). The time constants were determined by an efficient deconvolution routine (Porschke and Jung, 1985). Potential damage of the protein samples, including changes of the state of oxygenation during the measurements, were tested by taking UV spectra of the sample in the electrooptical cells in the range 380–480 nm before and after each experiment; in all cases, the absorbance did not change by more than 2–3%.

Calculations

Hydrodynamic simulations

Resistance and diffusion tensors (Brenner, 1965) were calculated according to the bead model approach described by Garcia de la Torre and Bloomfield

(1981), with a volume correction for calculation of rotational resistance coefficients (Garcia de la Torre and Rodes, 1983) as proposed by Antosiewicz and Porschke (1989b). Bead models of hemoglobin tetramers were constructed by substituting each amino acid by one bead. The center of each bead was located at the center of coordinates of the nonhydrogen atoms of the amino acid. For each amino acid, the distance between the bead center and the most remote atom was calculated; the average of these distances was increased by 2.8 Å to account for hydration, and the resulting value of 5.7 Å was used as bead radius. The increment for hydration results from the following considerations: hemoglobins may be approximated as spheres with radius 29.5 Å (see below). Their hydration is not greater than 0.36 g H_2O per g protein (Cantor and Schimmel, 1980), which may be represented by a layer of water $\leq$3.5 Å on the surface of the 29.5 Å sphere. Because this is a maximal estimate, we simply took one diameter of water molecule ($\approx$2.8 Å) as the depth of the hydration layer.

Each bead was treated as a friction center, having hydrodynamic interactions with each other bead. Our use of a single bead radius here was dictated by the fact that a hydrodynamic theory for the diffusion of overlapping beads exists only for beads of uniform radius (Garcia de la Torre and Bloomfield, 1981). Having diffusional tensors, Centers of Diffusion were calculated according to equations presented by Harvey and Garcia de la Torre (1980).

Calculation of extinction tensors

The dichroism of hemoglobin solutions was measured at 404.7 nm. Absorption of light in this wavelength range by hemoglobins is due to electronic transitions occurring in the heme groups. The absorption band around 400 nm is called the Soret or B band and is due to transitions polarized in the planes of heme chromophores (Eaton and Hofrichter, 1981). Thus, for each heme group its orientation was determined by a least-squares procedure that defines the plane with the lowest sum of squared deviations from the atoms of the porphyrine ring. In the local coordinate system, the x and y axes of each ring are in the plane, and in this system the extinction tensor of the heme is diagonal with $\epsilon^l_{xx} = \epsilon^l_{yy} = 1$ and $\epsilon^l_{zz} = 0$. The extinction of the whole protein molecule is taken as the tensorial sum of all subunit contributions, and the final result refers to the coordinate system in which the crystal structure is given.

Electrostatic calculations

The finite-difference Poisson-Boltzmann (FDPB) method (Warwicker and Watson, 1982; Klapper et al., 1986; Gilson et al., 1988; Davis et al., 1991) was used to calculate self energies and interaction energies of ionizable groups for a given ionic strength. The program UHBD (Davis et al., 1991) was used for all finite-difference calculations. Details of methodology involved in the use of the UHBD program in electrostatic calculations are described elsewhere (Antosiewicz et al., 1994), and only some basic points are presented here. For each ionizable group, a unit charge is placed at the protonation site and two sets of finite difference Poisson-Boltzmann calculations are performed. In the first, the dielectric environment is that of the entire protein; in the second, the dielectric environment is defined only by the residue containing the ionizable group (cf. Antosiewicz et al., 1994). These calculations are used to determine the local intrinsic pK_a of residues in the protein.

Atomic radii were set to 0.5 σ, where the σ values are those of the "OPLS nonbonded parameter set" (Jorgensen and Tirado-Rives, 1988). Because the OPLS parameters do not include charges for the neutral forms of each ionizable residue, these were taken from the CHARMm Version 22.0 (Brooks et al., 1982; Molecular Simulations Inc., 1992). Polar hydrogen atoms were added to Protein Data Bank files by means of the CHARMm HBUILD command (Brunger and Karplus, 1988). Ionization was represented by addition of $-$ or $+$ unit charges to the following atoms of different amino acid residues: C of main chain C-terminus; N of main chain N-terminus; CG of Asp; CD of Glu; CZ of Arg; NZ of Lys; NE2 of His; OH of Tyr; and SG of Cys, CDA and CDG of HEME group (notations according to the definition of the Protein Data Bank).

The following initial pK_a values were used: C-terminus 3.8; N-terminus 7.5; Asp 4.0; Glu 4.4; Arg 12.0; Lys 10.4; His 6.3; Tyr 9.6; Cys 8.3 (Nozaki and Tanford, 1967; Stryer, 1981), and heme propionic acid 4.0 (Matthew et al., 1979).

For all calculations, we used a temperature of 293 K, 10 mM (for deoxyhemoglobin) or 6 mM (for oxyhemoglobin) ionic strength of monovalent electrolyte with a 2.0 Å Stern layer and a solvent dielectric constant of 80. We used a dielectric constant of 15 for the protein. The high value of the dielectric constant of the protein should be regarded as operational parameter without physical meaning, as discussed elsewhere (Antosiewicz et al., 1994). The Richards probe accessible surface definition (Richards, 1977) of the dielectric surface was used with the probe sphere radius of 1.4 Å, and a starting set of 240 surface dots assigned to each atom-sphere (Gilson et al., 1988).

Calculations of dipole moments

Dipole moments of proteins may result from several different contributions. In general, dipole moments may be permanent, induced, or a sum of a permanent and an induced dipole moment. According to the available experimental data, the contribution of any induced dipole resulting from a polarizability of the protein appears to be relatively small (Porschke, 1987; Antosiewicz and Porschke, 1989a). For a description of their permanent electric moments, proteins may be considered as a set of electrical charges in a certain spatial arrangement. The dipole moment, **d**, of a charge distribution is defined (see, e.g., Böttcher, 1973) as

$$\mathbf{d} = \sum_i q_i \mathbf{r}_i, \tag{1}$$

where, r_j is the position vector of charge q_j in a coordinate system fixed to the particle.

Because of ion exchange with the environment, the charge configuration and, hence, the dipole moment vector of the macromolecule is fluctuating (Kirkwood and Shumaker, 1952; Scheider, 1965). There may be a second source of dipole moment fluctuations resulting from fluctuations in the macromolecular structure, which are not considered here. Our calculations of charge fluctuations are mainly concerned with protons and their binding to various sites on the protein, because there is a particularly large number of binding sites for protons in proteins. Thus, the binding of protons is described by a site-binding model. Some ions, for example, alkaline cations, may assume a certain average distribution around charged groups of polymers. There are also many cases of proteins that bind charged ions like Fe^{2+}, Ca^{2+}, Mn^{2+}, Mg^{2+}, Cu^{2+}, and Zn^{2+} to definite sites. In principle, all of these ions may contribute to the dipole moment of proteins. The Fe^{2+}-ion, which is localized at the center of the porphyrine group of each hemoglobin subunit, was included in our calculations by a contribution of two positive charges.

We note that fluctuations of protons between binding sites of a protein contribute to the permanent term of the whole dipole moment and not to the polarizability term (Scheider, 1965; Orttung, 1968; Antosiewicz and Porschke, 1993). However, it is possible that electric fields affect the distribution of protons among binding sites of the protein. This effect, which may contribute to a polarizability term, has not been considered in our calculations. In a previous investigation (Antosiewicz and Porschke, 1993), we have demonstrated that proton redistribution due to electric fields up to 100 kV/cm is negligible for the case of chymotrypsin. The field-induced proton redistribution is likely to be somewhat larger for hemoglobins because of their larger dimensions, but it is not expected to provide an essential contribution to the dipole. Before we enter into the details of our calculations on fluctuations in the next section, we describe the calculation of the dipole moment for a given protein state.

The calculation of a protein dipole moment according to Eq. 1 requires knowledge about values of all partial charges of its atoms in a given protonation state. These partial charges are not known unambiguously, but we think that the following two ways of calculating the dipole moment represent a reasonable approach to the problem. First, we may represent the total dipole as a sum of the following two contributions: 1) due to partial charges on atoms in the neutral state of all amino acids, and 2) due to changes in

charges of ionizable groups for a given protonation state relative to the neutral state. Charges of ionizable groups are assumed to be localized at certain atoms (see above). The dipole is given by

$$\mathbf{d} = \sum_{j=1}^{M} x_j \gamma_j \mathbf{r}_j + \mathbf{d}_{\text{neutral}}, \quad (2)$$

where summation over j counts only atoms representing ionizable sites, x_j is an ionization variable equal to 0 for neutral groups and 1 for ionized groups, and γ_j is the type of site equal to -1 for anionic sites and 1 for cationic sites.

As mentioned above, partial charges of the protein are not known unambiguously, but usually their contribution to the total protein dipole moment is small (Barlow and Thornton, 1986). However, it is known that peptide bonds in proteins are characterized by quite substantial dipole moments. Each peptide bond may be considered as a dipole of 3.5 Debye units directed from the C atom to the O atom of of the peptide group (Hol, 1985). The total dipole moment of peptide bonds is simply the vectorial sum of all contributions. Peptide bonds are known to contribute a substantial net dipole for α-helical fragments of proteins. Thus, as a second procedure for calculation of the dipole moment we have

$$\mathbf{d} = \sum_{j=1}^{M} x_j \gamma_j \mathbf{r}_j + \mathbf{d}_{\text{pb}}. \quad (3)$$

The dipole moment is independent of the origin of the coordinate system used for the calculation, when the whole molecule is neutral. However, dipole moments are dependent on the choice of the origin of the coordinate system used for the calculation, when the molecules bear a net charge. In this case, we calculate the dipole moment with respect to the center of diffusion of the protein as the appropriate origin of the coordinate system (cf. Harvey and Garcia de la Torre, 1980).

When the equilibrium distribution of protonation states is known, the above equations allow us to calculate mean and root-mean-square dipole moments of protein (see below). It is of interest to check whether the rather sophisticated procedures involved in computer simulations are really necessary. Thus, for each case we calculate also the dipole moments according to a "null" model. The null model implies that each ionizable site has a pK_a as given by the initial values listed above, and there is no electrostatic interaction between the sites. Finally, a comparison of total dipole moments calculated according to the various procedures allows us to get some information on the uncertainty in the calculation of the dipole moment resulting from the selection of a particular procedure.

Calculation of electrooptical parameters by a Monte Carlo procedure

The equilibrium distribution of ionization states of the protein at given pH, ionic strength, and temperature was generated by a Monte Carlo procedure (Metropolis et al., 1953). The Monte Carlo program used in the present work is a modification of a program described elsewhere (Antosiewicz and Porschke, 1989a). The previous version was based on the theory of Tanford and Kirkwood (1957); in the present version, local intrinsic pK_a values and energies of states are calculated from self energies and interaction energies for unit charges obtained by the finite-difference Poisson-Boltzmann method, as described above.

The program uses the Metropolis algorithm for sampling of protonation states (Metropolis et al., 1953). Generation of the equilibrium distribution is based on the free energy of a given state. The initial state is generated as follows: if the intrinsic pK_a values for ionizable sites are lower than the pH, then the site is assumed to be deprotonated; otherwise it is protonated. For this first sampled state of the protein, we calculate its Gibbs free energy ΔG_1. Subsequent states are sampled according to the following procedure: a change of the ionization state of each ionizable group is subject to a number from a uniform {0–1} random number generator: if the kth random number is larger than, e.g., 0.99, then the kth group changes its state of protonation; otherwise it remains unchanged. By this procedure, an average amount of 1% of the protein sites change their state in each Monte Carlo step. When the second state is generated, we calculate its free energy ΔG_2. If $\Delta G_2 \leq \Delta G_1$, then state 2 is accepted, and if $\Delta G_2 > \Delta G_1$, then state 2 is accepted with probability $\exp[(\Delta G_1 - \Delta G_2)/RT]$. Acceptance of the state 2 means that this state will be taken as the reference state in the next Monte Carlo step. If state 2 is rejected, state 1 is kept as the reference state. This procedure is continued, and the space of states is explored. Because the first sampled states may be far from the equilibrium, collection of states for equilibrium distributions is started after a sufficient number of initial Monte Carlo steps.

For each accepted state, the dipole moment of the protein is calculated according to Eq. 2 or 3. The program calculates also the limiting reduced dichroism for each accepted state. For this purpose, the extinction tensor is transformed to a system of axes where the z axis corresponds to the direction of the dipole moment and the limiting reduced dichroism is calculated according to

$$\left(\frac{\Delta\epsilon}{\epsilon}\right)_z = \frac{\epsilon_{zz} - (\epsilon_{xx} + \epsilon_{yy})/2}{Tr\epsilon/3}, \quad (4)$$

where $Tr\epsilon$ is the sum of diagonal elements of the tensor ϵ.

The dipole moments of individual states are used to calculate the mean dipole moment d_m, the root mean-square dipole moment d_{rms}, and the dipole moment fluctuation $\delta d = (d_{rms}^2 - d_m^2)^{1/2}$, arising from fluctuations in the occupancy of ionizable sites by protons. Finally, the mean reduced limiting dichroism and the reduced limiting dichroism in the direction of the mean dipole moment are calculated. The Monte Carlo calculations involved 10,000 initial sampling steps for equilibration followed by 100,000 sampling steps for generation of the equilibrium distribution of states.

Calculation of rotation time constants

As was shown by Wegener et al. (1979), force-free rotational diffusion motion of a particle of arbitrary shape and arbitrary symmetry with respect to its optical, electrical, and hydrodynamic properties is characterized by up to five relaxation times and amplitudes. These relaxation times and amplitudes are functions of components of the rotational diffusion tensor, the dipole moment vector, the polarizability tensor, and the optical extinction tensor.

For our calculations according to Wegener et al. (1979) we used mean dipole moments resulting from the FDPB evaluation and from the equilibrium distribution generated by the Monte Carlo procedure. The five relaxation times and amplitudes were subsequently used to generate sets of pseudo-experimental transient electrooptical data, which were evaluated like standard experimental data, i.e., exponentials were fitted by the program used for the evaluation of experimental decay curves.

Hemoglobin structures

The Protein Data Bank (Bernstein et al., 1977) provided coordinates for human deoxyhemoglobin (2HHB) (Fermi et al., 1984), human oxyhemoglobin (1HHO) (Shaanan, 1983), human deoxyhemoglobin S (1HBS) (Padlan and Love, 1985), and horse deoxyhemoglobin (2DHB) (Bolton and Perutz, 1970).

Technical data

For illustration and documentation of our calculations, we present some details and intermediate results, which may partly be compared with data available in the literature. An example of a bead model used for our simulations of the hydrodynamics is given in Fig. 1 for the case of human deoxyhemoglobin. The volume correction used for the calculation of rotational resistance coefficients is in the case of hemoglobins around 38,000 Å^3. The friction coefficients for translational motion (in units of 10^{-8} g/s) are: 6.04 for 2HHB, 5.99 for 1HHO, 6.02 for 1HBS, and 6.08 for 2DHB. This may be compared with a value 6.06 obtained from sedimentation measurements (Teller et al., 1979). The corresponding translational diffusion coefficients (in units of 10^{-7} cm^2/s) are 6.70, 6.75, 6.72, and 6.65, respectively, for the four hemoglobins. These values may be compared with an experimental value of 6.9 given by Cantor and Schimmel (1980).

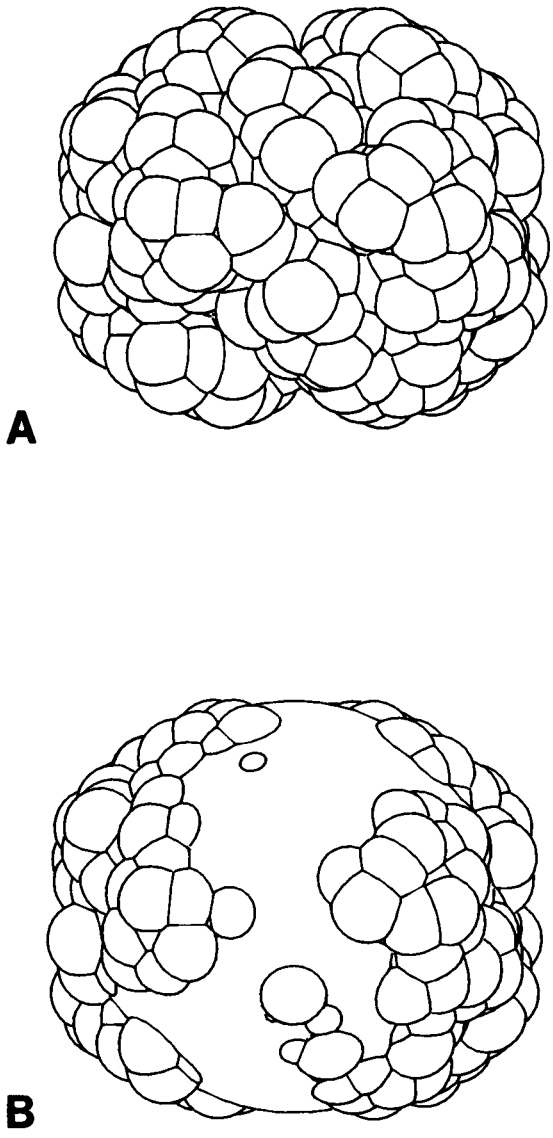

FIGURE 1 (*A*) Bead model of human deoxyhemoglobin; (*B*) the same model with a superimposed sphere of radius 30.3 Å, situated at the geometric center of the protein.

Hemoglobin Soret absorption ellipsoids are presented in Table 1. There are some differences in comparison with the values reported by Eaton and Hofrichter (1981), even for the same crystal structure data source (2DHB for horse deoxyhemoglobin). For human deoxyhemoglobin, we have used the 2HHB data in comparison with their 1HHB data. The reason for the differences is not known to us, because we do not have enough information about the calculation procedure used by Eaton and Hofrichter. The estimated planes of the porphyrine rings in our calculation result in root-mean-square deviations of the ring atoms not more than 0.8 Å in the case of the 2HHB, 1HHO, and 2DHB data. A particularly high value of the root-mean-square deviation (~1.6 Å) was found for the planes derived from the 1HBS data.

TABLE 1 Hemoglobins Soret absorption ellipsoids

Protein	$\epsilon_{xx}/\bar{\epsilon}$	$\epsilon_{yy}/\bar{\epsilon}$	$\epsilon_{zz}/\bar{\epsilon}$
2HHB	0.58	0.95	1.47
1HHO	0.63	0.88	1.49
1HBS	0.07	1.44	1.49
2DHB	0.56	0.97	1.47

Principal components of the extinction tensor relative to the mean extinction coefficient $\bar{\epsilon}$, given in the coordinate systems used in the data files of the Brookhaven Protein Data Bank.

RESULTS AND DISCUSSION

Electrooptical measurements

Electric field pulses applied on hemoglobin solutions induce optical effects, which are not only due to field-induced alignment, but also to chemical relaxation effects. The chemical relaxation effects are partly induced directly by the electric field pulse (cf. Bräunig et al., 1987), but appear to be mainly due to the change of temperature caused by the field pulse. In the present investigation, we are only interested in the field-induced alignment. Thus, the "side"-effects of chemical relaxation are kept at a minimal level by application of as short electric field pulses as possible. However, even then a small chemical relaxation amplitude persists for most hemoglobin samples. The chemical relaxation is detected selectively by measurements with light linearly polarized at the "magic angle" of 54.74° with respect to the vector of the external electric field. By this technique, two types of chemical relaxation responses have been found. The first one is associated with a time constant of more than 50 μs and has been found for all of the three hemoglobin samples used in the present investigation in their oxygenated state. Because this relaxation process is very slow with respect to the rotational correlation time (cf. below), it does not interfere with the field-induced alignment process, provided that the pulses are sufficiently short. The second process is reflected by a virtually linear decrease of the absorbance during the electric field pulse, which does not continue after pulse termination, and thus indicates a very fast relaxation. This fast process has been observed for all the three hemoglobin samples in their reduced state; its amplitude is small relative to the dichroism amplitudes for the horse and human standard hemoglobins. Because the dichroism amplitude for the sickle hemoglobin is particularly small, the influence of the fast chemical relaxation amplitude had to be eliminated by reading the dichroism amplitudes from the decay curves.

By avoiding side effects as described above, the stationary linear dichroism has been measured according to

$$\frac{\Delta\epsilon}{\bar{\epsilon}} = \frac{\Delta\epsilon_{\parallel} - \Delta\epsilon_{\perp}}{\bar{\epsilon}} = \frac{\Delta A_{\parallel} - \Delta A_{\perp}}{\bar{A}} = \frac{1.5 \cdot \Delta A_{\parallel}}{\bar{A}}, \qquad (5)$$

where $\Delta A_{\parallel}$ and $\Delta A_{\perp}$ are the absorbance changes measured with light polarized parallel and perpendicular with respect to the electric field vector; $\bar{A}$ is the isotropic absorbance; $\Delta\epsilon_{\parallel}$, $\Delta\epsilon_{\perp}$, and $\bar{\epsilon}$ are defined correspondingly for the extinction coefficients. Both oxygenated and deoxygenated forms of horse and human standard hemoglobins show positive values of the linear dichroism, whereas both forms of the sickle cell hemoglobin show a negative linear dichroism.

The stationary values of the linear dichroism were measured as a function of the electric field strength and fitted according to orientation functions for permanent and induced dipole moments. As shown in Fig. 2 for the case of horse

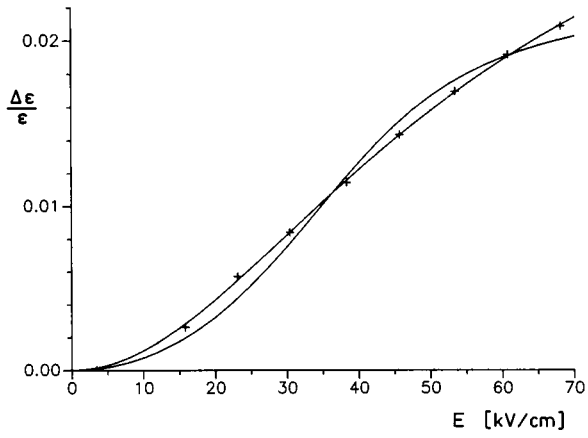

FIGURE 2 Reduced linear dichroism $\Delta\epsilon/\epsilon$ of horse oxyhemoglobin as a function of the electric field strength E. The solid line represents a least-squares fit of the data according to a permanent dipole mechanism with $\mu_p = 2.48 \times 10^{-27}$ Cm and $(\Delta\epsilon/\epsilon)_\infty = 0.044$. The dashed line represents a least-squares fit according to an induced dipole mechanism (10 mM Tris buffer + 100 μM $MgCl_2$, pH = 8.0, t = 2°C).

hemoglobin in its oxygenated form, the permanent dipole function fits the data very well within the limits of experimental accuracy, whereas the orientation function for induced dipoles cannot be used to represent the data. Similar results have been obtained for the other hemoglobin variants. In virtually all cases, the sum of the squared residuals found for the fits according to the orientation function for permanent dipoles was much smaller than that found for the induced dipole orientation function. From each set of experimental data, we get values for the permanent dipole moments and for the limit reduced dichroism, which are summarized in Table 2. The dipole moments have been corrected for the difference between the external and the internal directing electric field. According to the correction for spherical cavities in a medium with a high dielectric constant (approximately 80 for our case), the measured dipole moments have been reduced by a factor 1.5 (Böttcher, 1973).

TABLE 2 Summary of experimental data

Protein	$(\Delta\epsilon/\epsilon)_\infty$	d	τ
Human oxyhem.	0.09	260	62
	0.02	280	62
Human deoxyhem.	0.04	360	60
	0.03	260	54
Human S oxyhem.	−0.05	240	73
	−0.03	320	65
Human S deoxyhem.	−0.04	280	68
	−0.03	300	75
Horse oxyhem.	0.05	380	83
	0.06	340	91
Horse deoxyhem.	0.08	380	66
	0.08	400	72

Reduced limiting dichroisms, $(\Delta\epsilon/\epsilon)_\infty$, dipole moments, d (Debye units), and dichroism decay times, τ (ns). Dipole moments are corrected for cavity field effects, assuming a dielectric constant of the solvent 80.0 and a spherical cavity for the protein. Temperature, 2°C. For each protein, data in the first row refer to the buffer with 100 μM $MgCl_2$, and in the second to 500 μM $MgCl_2$. Estimated experimental errors: ±10% for τ and ±25% for $(\Delta\epsilon/\epsilon)_\infty$.

The dichroism decay curves have been measured at a high time resolution. Using an efficient deconvolution procedure, these curves could be represented by single exponentials at a high accuracy. The resulting relaxation time constants (cf. Table 2) show a considerable variation. The values may be compared with a reference value calculated for the rotational diffusion of a sphere with a radius of 32.3 Å (mean radius of hemoglobin "spheres" according to crystal structures with a correction term for hydration, cf. above). At 2°C in water this reference value is 62 ns. Some of the experimental relaxation times are larger, and others are smaller. Usually the larger values would be attributed to an elongated conformation of the protein, but our calculations (cf. below) indicate that the variation is not mainly due to changes of the shape.

The dichroism rise curves could not be characterized for all samples in both oxygenated and deoxygenated forms at a sufficient accuracy. This is partly due to interference with the "fast" chemical relaxation effect described above. In the case of the sickle cell hemoglobin, the amplitudes are relatively small and, thus, the signal-to-noise ratio is not sufficiently large for a quantitative analysis. The most accurate rise curves have been obtained for horse hemoglobin in the oxygenated form. Two exponentials, τ_1 and τ_2, according to

$$\Delta I = \Delta I_\infty \cdot \left(1 - \frac{\tau_1}{\tau_2 - \tau_1} \cdot e^{-t/\tau_1} - \frac{\tau_2}{\tau_2 - \tau_1} \cdot e^{-t/\tau_2}\right) \quad (6)$$

are required for fitting; ΔI and ΔI_∞ are the changes of the light intensity at time t and ∞, respectively. This equation describes rise curves with an initial zero slope (Porschke, 1985). Measurements at different electric field strengths E demonstrate that the rise time constants decrease with increasing E-values. A linear regression of the time constants τ_1 and τ_2 provides values at zero field strength, which are very close to the expectation for the case of permanent dipole moments (cf. Fig. 3). $\tau_1(E = 0) = 88 \pm 10$ ns is equivalent with the dichroism decay time constant τ_d, whereas $\tau_2(E = 0) = 220 \pm 20$ ns is equivalent with $3 \cdot \tau_d$. These equivalences are expected according to Benoit (1951) for perma-

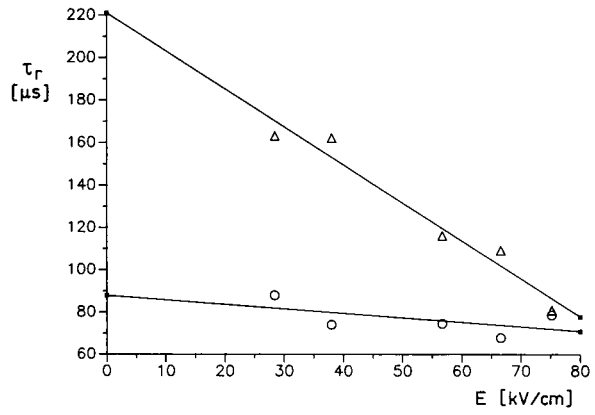

FIGURE 3 Risetimes constants τ_r^1 (○) and τ_r^2 (△) for horse hemoglobin in its oxygenated form as a function of the electric field strength E (2°C, 10 mM Tris pH 8.0, 500 μM $MgCl_2$). The straight lines represent linear regressions.

nent dipole moments in the limit of zero electric field strength. Thus, the results obtained from the dichroism rise curves confirm the conclusion on the existence of a permanent dipole moment derived from the stationary values of the dichroism.

Calculations

The results of our calculations according to the different models are compiled in various tables. The dipole moments and the corresponding values of the limiting reduced dichroism, calculated for conditions corresponding to those used in the experiments, are presented in Table 3. Table 4 presents results of calculations at isoelectric points. Table 5 shows electrooptical data for horse deoxyhemoglobin as a function of the pH.

The computations provide the following isoelectric points: 2HHB, 6.97; 1HHO, 6.72; 1HBS, 7.05; 2DHB, 6.83. These values are in good agreement with experimental values reported by Malamud and Drysdale (1978). The experimental value for human hemoglobin A is 7.0 and for hemoglobin S 7.3; other values from different sources are in the range 5.5–7.4.

A comparison of the data presented in Table 3 shows that the results for the two different models for the "neutral" state of the protein are only slightly different for the cases 2HHB, 1HHO, and 1HBS. In the case of 2DHB, the dipole moment calculated with the peptide dipole moments is clearly smaller than that obtained with consideration of all partial charges. It is not obvious why this effect is larger for 2DHB than for the other proteins.

The contribution of fluctuations is considerable for all hemoglobin species investigated. A particularly large fluctuation effect is found in the case of 2HHB, where the observed dipole moment is clearly dominated by proton fluctuations according to our calculations.

The calculated data are consistent with the experimental results in most cases, but there are also some deviations that are beyond the usual error limits. A particularly large deviation is found for the dichroism of 1HBS, where the calculated value is much larger than the experimental one. We do not have a simple explanation, but it is obvious that the dipole moments in the case of hemoglobins are relatively small and, thus, the directions of the calculated dipole vectors are subject to a relatively large uncertainty.

It should be of interest to illustrate the direction of the mean dipole moment. For this purpose, we show a ribbon model of human oxyhemoglobin (Fig. 4) within a given coordinate system and present the components of the dipole vector with respect to this coordinate system. The dipole components are also given for the other hemoglobin structures at a corresponding alignment of the molecules (cf. Table 6). For human oxy- and horse deoxyhemoglobins, the dominant contribution is in the direction of the y axis. For human deoxyhemoglobin S the dominant contribution is also in the direction of the y axis, but it is of opposite sign. In the case of human deoxyhemoglobin, the dipole is very small and is not preferentially directed in one of the major axes.

A special comment is required on the dichroism decay time constants. Usually these time constants are thought to be a measure of the size and shape of the molecules under investigation. The hemoglobin samples analyzed in the present investigation are very similar with respect to size and shape but, nevertheless, their dichroism decay time constants are quite different. Thus, there are factors in addition to size and shape with a strong influence on the dichroism decay. These factors can be clearly identified in the theoretical description given by Wegener et al. (1979). For objects without symmetry, the theory predicts five individual time constants, which are determined by the diffusion coefficients and, thus, are dependent on size and shape exclusively. However, the amplitudes of the relaxation processes contributing to the dichroism decay depend upon the dipole vector and the extinction tensor. A variation of the relative orientation of the dipole vector and the preferred axis of absorbance may have a particularly large influence, when individual amplitudes partially compensate each other and the stationary electric dichroism is small. For hemoglobins the stationary electric dichroism is close to zero in most cases and, thus,

TABLE 3 Calculated electrooptical data for pH 8.0, corresponding to experimental conditions

Protein	Null model		FDPB model				
	d_{nm}	$(\Delta\epsilon/\epsilon)_\infty^{nm}$	d_m	$(\Delta\epsilon/\epsilon)_\infty^{m}$	τ	d_{rms}	$(\Delta\epsilon/\epsilon)_\infty^{rms}$
Human oxi	118	−0.184	265	−0.184	64	312	−0.164
(1HHO)	125	−0.184	271	−0.184	64	318	−0.164
Human deoxy	43	−0.544	48	0.188	81	216	−0.084
(2HHB)	35	−0.532	45	0.004	52	216	−0.090
Human S deoxy	174	0.485	177	0.639	80	258	0.259
(1HBS)	183	0.493	185	0.634	80	264	0.273
Horse deoxy	550	−0.048	375	−0.050	43	441	−0.063
(2DHB)	607	−0.048	433	−0.049	43	490	−0.061

Null model: dipole moment, d_{nm}, and limiting reduced dichroism, $(\Delta\epsilon/\epsilon)_\infty^{nm}$. Finite-difference Poisson-Boltzmann method: mean dipole moment, d_m; root mean square dipole moment, d_{rms}; limiting reduced dichroism in the the direction of mean dipole moment, $(\Delta\epsilon/\epsilon)_\infty^{m}$; mean limiting reduced dichroism for all accepted states, $(\Delta\epsilon/\epsilon)_\infty^{rms}$. The values in the first line for each structure were calculated with the contribution from the sum of peptide bonds dipole moments as approximation of the dipole of the neutral form of the protein; in the second line, the dipole moments include contributions from partial charges of all atoms. Dipole moments are in Debye units. The dichroism decay time constant τ has been obtained from a least-squares exponential fit to the dichroism decay curve calculated for the respective protein using the mean dipole moment d_m. The data for the oxy-forms are given for pH 8.0, whereas the data for the deoxy-forms are given for pH 7.7

TABLE 4 Calculated electrooptical data for pH's corresponding to calculated isoelectric points

	Null model		FDPB model			
Protein	d_{nm}	$(\Delta\epsilon/\epsilon)_\infty^{nm}$	d_m	$(\Delta\epsilon/\epsilon)_\infty^{m}$	d_{rms}	$(\Delta\epsilon/\epsilon)_\infty^{rms}$
2HHB	74	−0.266	56	0.467	254	−0.038
	35	−0.254	51	0.403	252	−0.043
1HHO	27	−0.184	242	−0.182	352	−0.109
	34	−0.254	249	−0.182	357	−0.111
1HBS	217	0.503	111	0.667	257	0.020
	229	0.512	118	0.656	260	0.033
2DHB	459	−0.048	280	−0.047	386	−0.085
	516	−0.048	338	−0.047	429	−0.079

See Table 3 for symbols and other details.

TABLE 5 Calculated electrooptical data for horse deoxyhemoglobin as a function of pH

	Null model		FDPB model			
pH	d_{nm}	$(\Delta\epsilon/\epsilon)_\infty^{nm}$	d_m	$(\Delta\epsilon/\epsilon)_\infty^{m}$	d_{rms}	$(\Delta\epsilon/\epsilon)_\infty^{rms}$
5.0	57	−0.048	220	−0.051	335	−0.033
	1	−0.120	280	−0.050	375	−0.036
6.0	225	−0.048	265	−0.048	375	−0.048
	280	−0.048	320	−0.048	415	−0.050
7.0	490	−0.048	290	−0.049	400	−0.083
	545	−0.048	350	−0.049	445	−0.078
8.0	555	−0.048	420	−0.050	470	−0.060
	615	−0.048	480	−0.049	525	−0.058

Table 3 for symbols and other details.

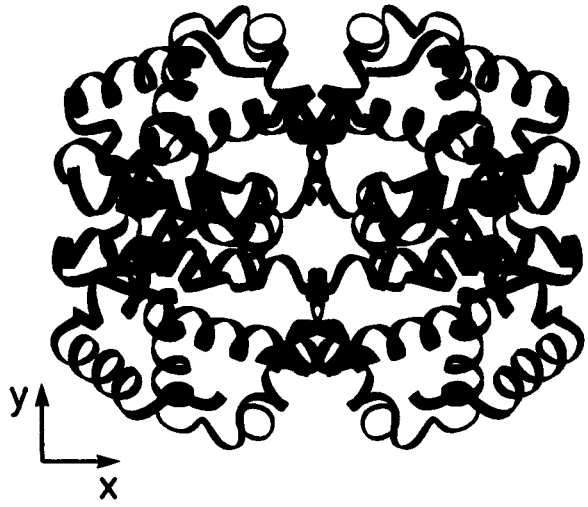

FIGURE 4 Ribbon model of human oxyhemoglobin (1HHO; Shaanan, 1983), given in the coordinate system used in the data file of the Brookhaven Protein Data Bank.

slight variations of the molecular structure may have a rather dramatic effect on the fitted decay time constant. This is illustrated by the examples given in Fig. 5. For 2DHB the calculations predict an exponential term with a large time constant and an amplitude opposite to that of the main terms; superposition of the components leads to a decay curve, which results in a particularly low time constant upon fitting by a single exponential. Usually the signal-to-noise ratio is not sufficient for an unequivocal identification of the individual contributions to dichroism decay curves.

TABLE 6 Components of the mean dipole vector d_m in the coordinate system corresponding to that used for 1HHO in Fig. 4

Protein	d_m^x	d_m^y	d_m^z
2HHB	19.2	−31.4	30.8
1HHO	−5.6	264.5	4.5
1HBS	58.9	−154.7	−62.5
2DHB	19.1	374.7	−8.2

The vector components for 2HHB, 1HHO, and 2DHB are in the coordinate system used in the data files of the Brookhaven Protein Data Bank; the components for 1HBS are given for an coordinate system, which leads to an orientation of 1HBS equivalent to that of the other molecules.

The experimental time constants are rather close to the predicted ones in most cases. A major deviation is found for 2DHB. In the case of 2HHB, the time constant according to the model including partial charges is in better agreement with the experimental result than the time constant obtained from the model based on peptide dipole moments. Thus, in this case small details of the model have a relatively large effect on the result.

A comparison with results of previous experimental and theoretical investigations

The dipole moment of hemoglobin has been studied previously by dielectric relaxation measurements. This procedure is based on measurements of dielectric constants of protein solutions as a function of the frequency of the applied electrical field. For evaluation of dipole moments from the experimental data, most authors use a calibration factor based on measurements for simple amino acids with known dipole

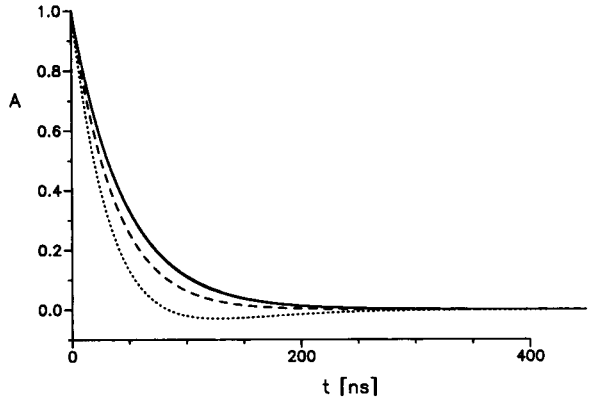

FIGURE 5 Dichroism decay curves calculated according to the crystal structures for the model with the mean dipole moment including the sum of peptide dipole moments. 1HBS and 2HHB (——, indistinguishable on the given scale), 1HHO (– – – –) and 2DHB (- - - - -).

moment. We have compiled the dipole moments obtained by this technique for several hemoglobin samples in Table 7. The values reported for different samples are in the range from ~300 to ~500 Debye units.

In general, the dielectric constants are measured in aqueous solutions without addition of salt or of buffer. Under these conditions, it is very difficult to control the pH of the solutions. Furthermore, the protein structure may not be native at the very low ionic strengths used for the measurements. Usually dielectric constants are measured at rather high protein concentration (1–140 mg/ml; cf. Takashima, 1993); specific dielectric increments are obtained by extrapolation to zero protein concentration. Despite the uncertainty resulting from various factors including extrapolation, some authors state a remarkably high accuracy (e.g., Takashima (1993) ±10 Debye units!).

TABLE 7 Experimental dipole moments obtained by dielectric increments measurements

Protein	Schlecht et al. (1968, 1969)	Takashima (1993)[a] or Goebel and Vogel (1964)[b]
Horse metHb	405	430[b]
Horse oxyHb	355	
Horse deoxyHb	340	
Human metHb A	325	
Human oxyHb A	308	479[a]
Human deoxyHb A	290	495[a]
Human oxyHb F	520	
Human deoxyHb F	490	
Human oxyHb S		
Human deoxyHb S		286[a]
Bovine metHb	310	

Dipole moments are in Debye units. (The data of Schlecht et al. were obtained at 16–17°C; estimated accuracy ±10%. The data of Goebel and Vogel were measured at 25°C. The data of Takashima refer to his values for deoxy-proteins measured at 25°C. All dielectric data were measured in water.)

For various reasons, it is very difficult to present a critical evaluation of the dipole moments obtained by dielectric relaxation measurements. For example, differences in the preparation of samples may have a strong influence on the result. Some authors do not specify the procedure for the preparation and/or control of deoxygenated samples; according to our experience, preparation of deoxygenated samples requires special caution. Under these conditions, a comparison of details in the experimental results does not make sense.

The first calculation of a dipole moment for hemoglobin has been reported by Orttung (1970). He used a multiple protonation equilibrium model (Orttung, 1968, 1969) derived on the theoretical basis provided by Tanford and Kirkwood (1957). According to his calculations for horse methemoglobin, the mean dipole moment increases in the pH range 6–8 from 180–325 Debye units; in the same pH range, the root-mean-square dipole moment increases from about 350 to 450 Debye units (data calculated for 25°C and 20 mM ionic strength). These calculated values are in very good agreement with the experimental data obtained by Goebel and Vogel (1964).

More recently, Takashima has presented calculations on the dipole moment of hemoglobin. He has calculated dipole moments at the isoelectric point, where the choice of the coordinate system does not influence the results under usual conditions. However, according to the equations given by Takashima for the calculation of the dipole moment, the distances between positive and negative charge centers were evaluated separately for each subunit and, thus, the dipole moment of each subunit refers to its "center." Because these subunits bear net charges, the calculated dipole moments include an artificial component. The artificial component would cancel out if the dipole moment for all subunits would be calculated with respect to the same reference point (provided that the *total* charge is zero). It is also conceivable that the error cancels out because of symmetry. However, according to control calculations using our programs, the error does not cancel in the case of hemoglobin. Although the subunits of hemoglobin molecules are arranged in a symmetry close to that of a tetrahedron, the symmetry is clearly not tetrahedral, which is obvious from the fact that hemoglobins contain two α and two β-subunits.

The error due to the artificial component resulting from the net charges of the subunits may be corrected. A simple derivation leads to the following expression for the relation between the dipole moment $\vec{\mu}$ calculated from the full charge distribution with respect to a given center and the dipole moment $\vec{\mu}'$ calculated as described by Takashima

$$\vec{\mu} = \vec{\mu}' + \sum_i q_i \vec{r}_i,$$

where q_i is the net charge of the ith subunit and $\vec{r}_i$ is the position of the reference point for the ith subunit with respect to the center of the whole molecule. Thus, the total

dipole moment can be obtained from the subunit moments referred to their centers, provided that contributions resulting from the net charges of the subunits are included.

The rotational diffusion of hemoglobin has been characterized previously by dielectric measurements. Schlecht et al. (1968, 1969) and Grant et al. (1971) used horse oxyhemoglobin and presented relaxation time constants of 132.5 ns at 17°C, 130 ns at 15°C, and 125 to 130 at 14.1°C. According to theory, the relaxation time constants obtained by electrooptical measurements are smaller than those obtained from dielectric relaxation measurements by a factor of three (cf. Fredericq and Houssier, 1973; Hill et al., 1969; McConnell, 1980). When this factor is considered and the time constants are also scaled to 2°C by the standard viscosity/temperature factor, we arrive at time constants for horse oxyhemoglobin between 63 and 72, which are clearly lower than the corresponding time constants obtained from our electrooptical measurements. The rotational diffusion of human oxyhemoglobin has been measured by paramagnetic resonance spectroscopy. McCalley et al. (1972) used a spin-labeled human oxyhemoglobin and found a rotational correlation time of 26 ns at 20°C. Scaling to 2°C provides a value of 46 ns, which is again clearly lower than that obtained by our electrooptical measurements. Part of the difference may be due to some mobility of the spin label. Probably the temperature has some influence on the structure and the mobility of the protein. Finally, some of the difference may be due to the different observation techniques, which may result in different contributions from the various modes of rotational diffusion to the measured signals (cf. above).

CONCLUSIONS

The combination of electrooptical experiments with computer simulations of charge distributions provides a sensitive test of the electrostatics of proteins. Electrooptical measurements are clearly more sensitive than dielectric ones, mainly because the optical anisotropy is obtained in addition to the dipole moment. The limiting electric dichroism is a measure for the orientation of the dipole moment relative to the axis of preferential light absorbance, which can be computed from crystal or model structures.

Hemoglobins prove to be relatively difficult for exact model calculations because of their size and because of the fact that the large number of ionizable sites is almost homogeneously distributed in the protein structure. Under these conditions, small deviations in the structure and/or in the state of ionization lead to relatively large changes of electrooptical parameters. Thus, hemoglobins provide a useful test for the state of the art of electrostatic model calculations. Although some deviations between experiments and calculations remain, a satisfactory agreement in most cases indicates that the electrostatics of proteins may be simulated at a high degree of accuracy.

The advice of Prof. Dr. G. Ilgenfritz, Prof. Dr. W. E. Love, and Dr. H. J. Steinhoff is gratefully acknowledged. We also thank the referees for their comments.

The computations using the UHBD and Monte Carlo programs at the University of Houston were supported in part by a National Institutes of Health grant to Prof. J. A. McCammon. All of the other calculations were performed on the facilities of the Gesellschaft für wissenschaftliche Datenverarbeitung mbH, Göttingen. Model drawings were prepared by the program SHAKAL written by E. Keller.

REFERENCES

Antosiewicz, J., and J. A. McCammon, M. K. Gilson. 1994. Theoretical prediction of pH-dependent properties of proteins. *J. Mol. Biol.* 238: 415–436.

Antosiewicz, J., and D. Porschke. 1989a. The nature of protein dipole moments: experimental and calculated permanent dipole of α-chymotrypsin. *Biochemistry.* 28:10077–10078.

Antosiewicz, J., and D. Porschke. 1989b. Volume correction for bead model simulations of rotational friction coefficients of macromolecules. *J. Phys. Chem.* 93:5301–5305.

Antosiewicz, J., and D. Porschke. 1993. Brownian dynamics simulation of electrooptical transients for complex macrodipoles. *J. Phys. Chem.* 97: 2767–2773.

Barlow, D. J., and J. M. Thornton. 1986. The distribution of charged groups in proteins. *Biopolymers.* 25:1717–1733.

Benoit, H. 1951. Contribution a l'étude de l'effect kerr présenté par les solutions diluées de macromolécules rigides. *Ann. de Phys.* 6:561–609.

Bernstein, F. C., T. F. Koettzle, G. J. B. Williams, E. F. Meyer, Jr., M. D. Brice, J. R. Rodgers, O. Kennard, T. Shimanouchi, and M. J. Tasumi. 1977. The protein data bank: a computer-based archival file for molecular structures. *J. Mol. Biol.* 123:557–594.

Bolton, W., and M. F. Perutz. 1970. Three dimensional Fourier synthesis of horse deoxyhaemoglobin at 2.8 Angstroms resolution. *Nature.* 228:551–552.

Böttcher, C. J. F. 1973. Theory of Electric Polarization, Vol. 1. Elsevier, Amsterdam.

Bräunig, R., Y. Gushimana, and G. Ilgenfritz. 1987. Ionic strength dependence of the electric dissociation field effect. Investigation of 2,6-dinitrophenol and application to the acid-alkaline transition of metmyoglobin and methemoglobin. *Biophys. Chem.* 26:181–191.

Brenner, H. 1965. Coupling between the translational and rotational brownian motions of rigid particles of arbitrary shape. *J. Colloid Sci.* 20:104–122.

Brooks, B. R., R. E. Bruccoleri, B. D. Olafson, D. J. States, S. Swaminathan, and M. Karplus. 1982. CHARMm: a program for macromolecular energy, minimization, and dynamics calculations. *J. Comput. Chem.* 4:187–217.

Brunger, A. T., and M. Karplus. 1988. Polar hydrogen positions in proteins: empirical energy placement and neutron diffraction comparison. *Proteins Struct. Funct. Genet.* 4:148–156.

Cantor, C. R., and P. R. Schimmel. 1980. Biophysical Chemistry, Part 2. W. H. Freeman and Company, San Francisco, CA.

Davis, M. E., J. D. Madura, B. A. Luty, and J. A. McCammon. 1991. Electrostatics and diffusion of molecules in solution: simulations with the University of Houston Brownian dynamics program. *Comp. Phys. Commun.* 62:187–197.

Di Iorio, E. E. 1981. Preparation of derivatives of ferrous and ferric hemoglobin. *Methods. Enzymol.* 76:57–72.

Eaton, W. A., and J. Hofrichter. 1981. Polarized absorption and linear dichroism spectroscopy of hemoglobin. *Methods Enzymol.* 76:175–261.

Fermi, G., M. F. Perutz, B. Shaanan, and R. Fourme. 1984. The crystal structure of human deoxyhaemoglobin at 1.74 Angstroms resolution. *J. Mol. Biol.* 175:159–174.

Fredericq, E., and C. Houssier. 1973. Electric Dichroism and Electric Birefringence. Clarendon Press, Oxford.

Garcia de la Torre, J., and V. A. Bloomfield. 1981. Hydrodynamic properties of complex, rigid, biological macromolecules: theory and applications. *Q. Rev. Biophys.* 14:81–139.

Garcia de la Torre, J., and V. Rodes. 1983. Effects from bead size and hydrodynamic interactions on the translational and rotational coefficients of macromolecular bead models. *J. Chem. Phys.* 79:2454–2460.

Gilson, M. K., K. A. Sharp, and B. H. Honig. 1988. Calculating the electrostatic potential of molecules in solution: method and error assessment. *J. Comput. Chem.* 9:327–335.

Goebel, W., and H. Vogel. 1964. Dielektrische Eigenschaften von Hämoglobin und Ursachen ihrer Entstehung I. *Z. Naturforschg.* 19B: 292–302.

Grant, E. H., R. J. Sheppard, and G. P. South. 1978. Dielectric Behaviour of Biological Molecules in Solution. Clarendon Press, Oxford. 207–213.

Grünhagen, H. H. 1974. Entwicklung einer E-Feldsprung-Apparatur mit optischer Detektion und Ihre Anwendung auf die Assoziation amphiphiler Electrolyte. Ph.D. thesis. Universität Braunschweig.

Harvey, S. C., and J. Garcia de la Torre. 1980. Coordinate systems for modeling the hydrodynamic resistance and diffusion coefficients of irregularly shaped rigid macromolecules. *Macromolecules.* 13:960–964.

Hill, N. A., W. E. Vaughan, A. H. Price, and M. Davies. 1969. Dielectric Properties and Molecular Behaviour. Van Nostrand, London.

Hol, W. G. J. 1985. The role of the α-helix dipole in protein function and structure. *Prog. Biophys. Mol. Biol.* 45:149–195.

Jorgensen, W. L., and J. Tirado-Rives. 1988. The OPLS potential function for proteins. Energy minimizations for crystals of cyclic peptides and crambin. *J. Am. Chem. Soc.* 110:1657–1666.

Kirkwood, J. G., and J. B. Shumaker. 1952. The influence of dipole moment fluctuations on the dielectric increment of proteins in solutions. *Proc. Natl. Acad. Sci. USA.* 38:855–862.

Klapper, I., R. Hagstrom, R. Fine, K. Sharp, and B. Honig. 1986. Focusing of electrostatic fields in the active site of Cu, Zn superoxide dismutase. *Proteins Struct. Funct. Genet.* 1:47–79.

Malamud, D., and J. W. Drysdale. 1978. Isoelectric points of proteins: a table. *Anal. Biochem.* 86:620–647.

Matthew, J. B., G. I. H. Hanania, and F. R. N. Gurd. 1979. Electrostatic effects in hemoglobin. I. Hydrogen ion equilibria in human deoxy- and oxyhemoglobin A. *Biochemistry.* 18:1919–1928.

McCalley, R. C., E. J. Shimshick, and H. M. McConnel. 1972. The effect of slow rotational motion on paramagnetic resonance spectra. *Chem. Phys. Lett.* 13:115–119.

McConnell, J. 1980. Rotational Brownian Motion. Academic Press, London.

Metropolis, N., A. W. Rosenbluth, M. N. Rosenbluth, A. H. Teller, and E. Teller. 1953. Equation of state calculations by fast computing machines. *J. Chem. Phys.* 21:1087–1092.

Molecular Simulations Inc. 1992. Polar Hydrogen Parameter set for CHARMm, Version 22. Waltham, MA.

Nozaki, Y., and C. Tanford. 1967. Examination of titration behavior. *Methods Enzymol.* 11:715–734.

O'Konski, C., K. Yoshioka, and W. H. Orttung. 1959. Electric properties of macromolecules. IV. Determination of electric and optical parameters from saturation of electric birefringence in solutions. *J. Phys. Chem.* 63: 1558–1565.

Oncley, J. J. 1943. The electric moments and the relaxation times of proteins as measured from their influence upon the dielectric constants of solutions. *In* Proteins, Amino Acids and Peptides. J. J. Cohn and J. T. Edsall, editors. American Chemical Society Monograph Series.

Onsager, L. 1936. Electric moments of molecules in liquids. *J. Am. Chem. Soc.* 58:1486–1493.

Orttung, W. H. 1968. Anisotropy of proton fluctuations and the Kerr effect of protein solutions. Theoretical considerations. *J. Phys. Chem.* 72:4058–4066.

Orttung, W. H. 1969. Calculation of the mean-square dipole moment and proton fluctuation. *J. Phys. Chem.* 73:418–423.

Orttung, W. H. 1970. Proton binding and dipole moment of hemoglobin. Refined calculation. *Biochemistry.* 9:2394–2402.

Padlan, E. A., and W. E. Love. 1985. Refined crystal structure of deoxyhaemoglobin S. I. Restrained least-squares refinement at 3.0 Angstroms resolution. *J. Biol. Chem.* 260:8272–8279.

Porschke, D. 1980. Structure and dynamics of a tryptophanpeptide-polynucleotides complex. *Nucleic Acids Res.* 8:1591–1612.

Porschke, D. 1985. The mechanism of ion polarization along DNA double helices. *Biophys. Chem.* 22:237–247.

Porschke, D. 1987. Electric, optical and hydrodynamic parameters of lac repressor from measurements of the electrical dichroism. High permanent dipole moment associated with the protein. *Biophys. Chem.* 28:137–147.

Porschke, D., and M. Jung. 1985. The conformation of single stranded oligonucleotides and of oligonucleotide-oligopeptide complexes from their rotation relaxation in the nanosecond time range. *J. Biomol. Struct. Dyn.* 2:1173–1184.

Porschke, D., H. J. Meier, and J. Ronnenberg. 1984. Interactions of nucleic acid double helices induced by electric field pulses. *Biophys. Chem.* 20: 225–235.

Richards, F. M. 1977. Areas, volumes, packing and protein structure. *Annu. Rev. Biophys. Bioeng.* 6:151–176.

Scheider, W. 1965. Dielectric relaxation of molecules with fluctuating dipole moment. *Biophys. J.* 5:617–628.

Schlecht, P., A. Mayer, G. Hettner, and H. Vogel. 1969. Dielectric properties of hemoglobin and myoglobin. I. influence of solvent and particle size on the dielectric dispersion. *Biopolymers.* 7:963–974.

Schlecht, P., H. Vogel, and A. Mayer. 1968. Effect of oxygen binding on the dielectric properties of hemoglobin. *Biopolymers.* 6:1717–1725.

Shaanan, B. 1983. Structure of human oxyhaemoglobin at 2.1 Angstroms resolution. *J. Mol. Biol.* 171:31–59.

Stryer, L. 1981. Biochemistry, 2nd ed. W. H. Freeman and Co., San Francisco, CA.

Takashima, S. 1993. Use of protein database for the computation of the dipole moments of normal and abnormal hemoglobins. *Biophys. J.* 64: 1550–1558.

Tanford, C., and J. G. Kirkwood. 1957. Theory of protein titration curves. I. General equations for impenetrable spheres. *J. Am. Chem. Soc.* 79: 5333–5339.

Teller, D. C., E. Swanson, and C. de Haen. 1979. The translational friction coefficient of proteins. *Adv. Enzymol.* 61:103–124.

Warwicker, J., and H. C. Watson. 1982. Calculation of the electric potential in the active site cleft due to α-helix dipoles. *J. Mol. Biol.* 157:671–679.

Wegener, W. A., R. M. Dowben, and V. J. Koester. 1979. Time-dependent birefringence, linear dichroism, and optical rotation resulting from rigid-body rotational diffusion. *J. Chem. Phys.* 70:622–632.